*Desalination and Water Treatment*
www.deswater.com

doi: 10.5004/dwt.2017.21808

100 (2017) 38–45
December

# Phenol degradation using adsorption methods, advanced oxidative process ($H_2O_2$/UV) and $H_2O_2$/UV/activated carbon coupling: influence of homogeneous and heterogeneous phase

Michelly Freitas de Moraes[a,*], Tatianne Ferreira de Oliveira[a], Jorge Cuellar[b], Gabriel Luis Castiglioni[a]

[a]*School of Agronomy, Federal University of Goias - UFG Campus Samambaia, Rodovia Goiania-Nova Veneza, Km 0- Caixa Postal 131, CEP 74690-900, Goiania, Brazil, Tel. +55 6239913922, email: michelly_moraes_@hotmail.com (M.F. de Moraes), Tel. +55 6235211613, email: ferreira.tatianne@yahoo.com.br (T.F. de Oliveira), Tel. +55 6235211616, email: gabrielcastigli@gmail.com (G.L. Castiglioni)*
[b]*Department of Chemical Engineering, University of Salamanca, Plaza de los Caidos 1-5, 37008 Salamanca, Spain, Tel. +34923294479, email: cuellar@usal.es*

Received 2 June 2017; Accepted 11 December 2017

**ABSTRACT**

The aim of this study was to evaluate the efficiency of UV/$H_2O_2$/AC coupling processes and adsorbent behavior in coupling to eliminate phenol. Activated carbon was characterized for the textural analysis by isotherms of $N_2$ adsorption and desorption at 77K, Scanning Electron Microscopy, infrared spectroscopy, elemental analysis, Boehm's method and point of zero charge. Adsorption kinetics was performed for each 11 tests, according to the experimental design $2^3$ + 3 central points, in which there were variations in pH, temperature and the quantity of activated carbon. The pseudo-second order model was the one that best represented the adsorption process. The best tests for $H_2O_2$/UV and $H_2O_2$/UV/AC processes were the central points with phenol elimination rates of 89% and 94%, respectively. The kinetic contribution of the hydroxyl radicals was calculated with the presence of tert-butanol showing that 78% of phenol elimination in the $H_2O_2$/UV/AC treatment was caused by their action. The $H_2O_2$/UV/AC coupling process is acceptable and presents a higher removal rate than the adsorption process with much shorter removal time.

*Keywords:* Kinectics modeling; Tert-butanol; Coupling; Adsortion

## 1. Introduction

Petrochemical, gasification, coal carbonization, pharmaceutical, wood preservation chemicals, plastics, pesticides, paper and cellulose industries generate highly toxic and carcinogenic phenolic substances [1]. Phenolic compounds are very harmful to humans and animals, even at low concentrations [2]. According to the World Health Organization (WHO), the allowed concentration of phenolic content in drinking water is 1 $\mu g \cdot L^{-1}$, depending on the compound.

Strict environmental standards have brought remediation technologies for phenol removal such as biological treatment, oxidation, adsorption, etc. However, the adsorption process is one of the most used techniques for treatment of contaminated water contaminated due to its low operational cost, adsorbent availability and high efficiency [3].

In this context, advanced oxidative processes (AOP) are very efficient in contaminated soils and water. AOP can also lead to other contaminants formation, as oxygenated organic compounds and low molecular weight organic acids which can be applied in the treatment of contaminated water with low concentration of pollutants [4].

Since there are almost no reports about adsorption coupling using activated carbón and due to the need of having

*Corresponding author.

more efficient technologies in phenol elimination in effluents, the aim of this study was to evaluate the process efficiency and the adsorbent behavior in UV/$H_2O_2$/activated carbon coupling in the elimination of phenol. The pH (3, 7 and 11), temperature (15°C, 30°C and 45°C) and activated carbon mass (0.2, 0.4 and 0.6 g) were evaluated.

## 2. Materials and methods

### 2.1. Activated carbon characterization

Activated carbon was donated by FBC (Fábrica Brasileira de Catalisadores, Brazil). Textural analysis was performed on a porosimeter (MICROMERITICS, model Gemini V2380). Specific surface area ($m^2 \cdot g^{-1}$) was measured through BET method (Brunauer, Emmet and Teller). Total pore volume ($cm^3 \cdot g^{-1}$), micropore volume ($cm^3 \cdot g^{-1}$), size distribution and average pore diameter (Å) were estimated from the linear part of the Dubinin-Radushkevich plot [5,6]. Boehm method was performed to determine surface functional groups (acids and basic) [7]. Point of zero charge ($pH_{PZC}$) was obtained through the method proposed by [8]. Adsorption spectra in the infrared region was obtained using a spectrophotometer (PERKINELMER, model Spectrum 400). Analyzes were concentrated in the infrared region between 4000 and 400 $cm^{-1}$ with a resolution of 4 $cm^{-1}$. SEM analyzes were performed using an Electron Scanning Electron Microscope (JEOL, model JSM – 6610) aiming at evaluating activated carbon.

### 2.2 Adsorption with activated carbon

Eleven tests were performed in a complete factorial design $2^3$ with 3 replicates at the central point. The following parameters were analyzed: pH (3, 7 and 11), temperature (15, 30 and 45°C) and activated carbon mass (0.2, 0.4 and 0.6 g). Activated carbon samples were placed in contact with 150 mL 0.2 $g \cdot L^{-1}$ phenol buffer under constant stirring at 200 rpm for 24 h in an incubator (TECNAL, model TE-4200). Aliquots of 10 mL were collected at the following times: 0, 5, 15, 25, 35, 45, 60, 80, 100, 120, 150, 180, 210, 240, 360, 1290, 1380 and 1440 min. After each collection, samples were filtered with 25 µm qualitative filter paper and subjected to analysis on a UV-visible spectrophotometer (FEMTO, 700 plus) at λ = 265 nm. After kinetics and statistical analysis, the best condition (pH and activated carbon mass) to perform the isotherms was chosen. Three isotherms were perfomed (15°C, 30°C and 45°C), each one with eight initial phenol concentrations. The analyzes were performed in triplicate.

#### 2.2.1. Mathematical modeling

Kinetic modeling was performed using pseudo-first order model [9] represented by Eq. (1); pseudo-second order [10] [Eq. (2)] and intraparticle diffusion [11] [Eq.(3)].

$$\frac{dq_t}{dt} = k_1\left(q_e - q_t\right) \quad (1)$$

$$\frac{dq_t}{dt} = k_2\left(q_e - q_t\right)^2 \quad (2)$$

$$q_t = k_3 t^{0,5} + c \quad (3)$$

In which $q_e$ is the amount of solute adsorbed per unit of adsorbent mass ($mg \cdot g^{-1}$); $q_t$ is the amount of solute adsorbed per unit of adsorbent mass ($mg \cdot g^{-1}$) at time t (min); $k_1$ is the kinetic constant of pseudo-first order ($min^{-1}$); $k_2$ is the kinetic constant of pseudo-second order ($g \cdot mg^{-1} \cdot min^{-1}$); $k_3$ is the intraparticle diffusion kinetic constant ($mg \cdot g^{-1} \cdot min^{-0.5}$) and $c$ is the constant related to the thickness of the internal or external diffusion layer ($mg \cdot g^{-1}$).

### 2.3. $H_2O_2$/UV

A complete factorial design $2^2$ was performed with 3 replicates at the central point, totaling 7 tests in each, under the incidence of 33 W of UV-C. The following parameters were analyzed: pH (3, 7 and 11) and $H_2O_2$ concentration (10, 20 and 30 mmol). 150 mL of 0.2 g $L^{-1}$ phenol buffer solution was placed in each erlenmeyer under constant stirring at 200 rpm on a magnetic stirrer (FISATOM, model 752) for 2 h at a constant temperature of 30°C and submitted to ultraviolet radiation (UV-C) emitted by three 11 W light bulbs, totaling 33 W, located 10 cm from the solution surface. Aliquots of 10 mL were collected at the following times: 0, 6, 12, 24, 36, 48, 60, 80, 80, 100 and 120 min. After each collection, 5 mL of sodium sulfite (0.1 $mol \cdot L^{-1}$ $Na_2SO_3$) was added to cease the oxidation reaction and was analyzed by a chromatograph (SHIMADZU, model LC 8A) at 265 nm.

Regression coefficients and p-values were determined using the Statistica 7.0 program and it was determined which factors and interactions were significant at 5%.

### 2.4. $H_2O_2$/UV/activated carbon coupling

A complete factorial design $2^2$ was performed, with 3 replicates at the central point, totaling 7 tests in each, varying pH (3, 7 and 11) and $H_2O_2$ concentration (10, 20 and 30 mmol) with 0.6 g activated carbon under UV-C 33 W. 150 mL of buffer containing 0.2 $g \cdot L^{-1}$ of phenol and 0.6 g activated carbon were placed in each erlenmeyer flask under constant stirring at 200 rpm on a magnetic stirrer (FISATOM, model 752), for 2 h at 30°C and subjected to ultraviolet (UV-C) radiation emitted by three 11 W light bulbs, totaling 33 W, located 10 cm from the solution surface.10 mL aliquots were collected at the following times: 0, 6, 12, 24, 36, 48, 60, 80, 100 and 120 min. After each collection, 5 mL of sodium sulfite (0.1 $mol \cdot L^{-1}$ $Na_2SO_3$) was added to cease the oxidation reaction and they were analyzed by a chromatograph (SHIMADZU, model LC 8A) at 265 nm.

Regression coefficients and p-values were determined using Statistica 7.0 program and it was determined which factors and interactions were significant at 5%.

### 2.5. $H_2O_2$/UV/activated carbon/tert-butanol coupling

The experimental procedure was performed as in the UV/$H_2O_2$/AC coupling process, with the addition of free radical inhibitor (tert-butanol), in which the inhibitior's

concentration was 30 times higher than phenol's to verify the influence of OH radical, as proposed by [12].

### 2.6. Kinetic model of $H_2O_2$/UV, $H_2O_2$/UV/AC and $H_2O_2$/UV/AC/tert-butanol

The direct or indirect degradation of phenol can be expressed by the following equation:

$$-\ln\frac{[phenol]_{final}}{[phenol]_{initial}} = k_{homogeneous}\cdot t \quad (4)$$

Thus, $k_{homogeneous}$ is the slope of Eq. (4) and represents the first-order kinetic constant for the reaction rate in $H_2O_2$/UV treatment (in the absence of activated carbon).

$k_{global}$ represents the global reaction constant in the heterogeneous phase (in the presence of activated carbon) [Eq. (5)] and homogeneous:

$$-\ln\frac{[phenol]_{final}}{[phenol]_{initial}} = k_{global}\cdot t \quad (5)$$

The determination of $k_{global}$ allows to calculate the kinetic constant of the heterogeneous reaction ($k_{heterogeneous}$) by Eq. (6), $\delta_{homogeneous}$ and $\delta_{heterogeneous}$ according to Eqs. (6), (7) and (8):

$$k_{global} = k_{homogeneous} + k_{heterogeneous} \quad (6)$$

$$\delta_{homogeneous} = \frac{k_{homogeneous}}{k_{global}}\cdot 100 \quad (7)$$

$$\delta_{heterogeneous} = \frac{k_{heterogeneous}}{k_{global}}\cdot 100 \quad (8)$$

For the experiments with $H_2O_2$/UV/AC/tert-butanol, radical reactions were eliminated and the equation can be simplified by:

$$-\ln\frac{[phenol]_{final}}{[phenol]_{initial}} = k_{globalobs}\cdot t \quad (9)$$

With the determination of $k_{global}$ and $k_{global\ obs}$ by Eqs. (5) and (9), respectively, it is possible to estimate the kinetic contribution of the radical reactions in the degradation of phenol ($\delta_{OH}$°), according to Eq. (10):

$$\delta_{OH^\circ} = \frac{k_{global} - k_{globalobs}}{k_{global}}\cdot 100 \quad (10)$$

### 2.7. Adsorbate analysis

Samples from the adsorption processes were analyzed by spectrophotometer (FEMTO, model 700 plus) in the ultraviolet region, with λ = 265 nm. A chromatograph (SHIMADZU, model LC 8A) was used to determine phenol in the $H_2O_2$/UV, $H_2O_2$/UV/Activated carbon and $H_2O_2$/UV/activated carbon/tert-butanol processes using a diode arrangement detector (SHIMADZU, Model SPD 20A), with the system in 265 nm in isocratic mode and C-18 (SGE, WAKOSIL) reverse phase (5 µm, 4.6 mm × 250 mm). The mobile phase consisted of an aqueous solution of 70% acetonitrile and 30% ultra pure water, with flow rate of 1 mL·min$^{-1}$ and manual injection of 25 µL sample.

## 3. Results and discussion

### 3.1. Activated carbon characterization

Chemical properties of activated carbon are shown in Table 1. Boehm titration determined that activated carbon is composed of more basic groups than acid ones. The basic behavior was confirmed by determining the point of zero charge value (pHPZC = 7.3). Infrared analysis result is consistently compared to Boehm method and pHPZC. In the infrared spectrum, represented by Fig. 1, there is a broadband with frequency at 3433 cm$^{-1}$ (–OH), peaks at 2926 cm$^{-1}$ and 2854 cm$^{-1}$ (CH), elongation at 1630 cm$^{-1}$ (C=C) in alkanes, band at 1455 cm$^{-1}$ ($CH_2$) of the pyran ring and peak with frequency at 1091 cm$^{-1}$ (CO) [13]. CHN elemental analysis was performed and the results were 75.3% C, 0.6% H, 0.7% N and 23.4% O. Micropore volume represents 77.63% total pores of the activated carbon, showing that the activated carbon is predominantly microporous.

Table 1
Textural and chemical characteristics of the activated carbon

| | |
|---|---|
| Total pore volume (cm$^3$/g) | 0.29 |
| Micropore volume (cm$^3$/g) | 0.23 |
| Superficial area BET (m$^2$/g) | 512 |
| Average pore diameter (Å) | 20.79 |
| Point of zero charge $pH_{PZC}$ | 7.27 |
| Basic groups (mEq·g$^{-1}$) | 2.55 |
| Acid groups (mEq·g$^{-1}$) | 0.05* |

*Composed only of carboxylic groupswithout phenolic and lactonic groups

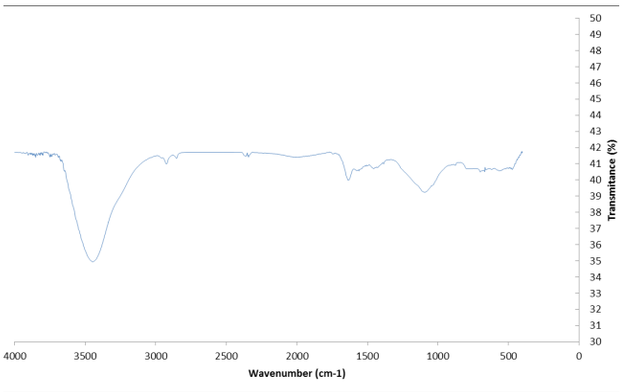


Fig. 1. Spectrum in the infrared region of crude activated carbon. KBr pellets experiment.

### 3.2. Phenol kinetic degradation

#### 3.2.1. Adsorption with activated carbon

A complete factorial design $2^3$ was performed, with 3 replicates at the central point, totaling 11 tests for the adsorption process (Table 2). Adsorption capacity was calculated from each adsorption kinetics and it was used as parameter to evaluate the tests (Table 2).

Tests 9, 10 and 11 obtained different results due to possible influence of equipment used and perhaps by analytical error, since the test conditions were the same.

##### 3.2.1.1. Effect of adsorbent mass, pH and temperature

Analyzing Table 2, it was possible to determine the process conditions with the best performance. The highest value for adsorption capacity was obtained in test 7 (with the highest temperature, highest pH and lowest mass). The $q$, calculated according to Eq. (11), can be influenced by several experimental parameters such as temperature, volume, inicial pollutant concentration, pH, rotation, relation between pollutant concentration and activated carbon mass, as well as adsorbent material properties. Condition 8 was the chosen one, with adsorption capacity of 30.79 mg/g. Similar results for $q_{max}$ (38 mg/g) were obtained by [14].

$$q_e = \frac{(C_0 - C_e)\cdot V}{M} \tag{11}$$

In which, $q_e$ is the amount of solute adsorbed by unit of adsorbent mass ($mg\cdot g^{-1}$), $C_0$ and $C_e$ ($mg\cdot L^{-1}$) are the initial and final concentrations of the adsorbent in the liquid phase, respectively. $V$ is the solution volume (L) and $M$ is the adsorbent mass (g).

Phenol is considered as a weak acid (pKa = 9.89) and, consequently, it is adsorbed at higher pH values due to the repulsive force [14]. The zero charge point is the pH where a surface charge of the adsorbent corresponds to zero, and offers the possible mechanism over an electrostatic interaction between adsorbent and adsorbate. The pHPZ Cobtained for the activated carbón was 7.27. The activated carbon surface is positively charged at pH less than 7.27. When pH rises from 3 to 11 under the same conditions, the adsorption capacity increases from 45.2 $mg\cdot g^{-1}$ (test 5) to 67.4 $mg\cdot g^{-1}$ (test 7), as shown in Table 2. This occurs as a consequence of the increase of electrostatic interactions between phenol cationic substances due to the deprotonation of surface active sites [16]. Increasing temperature, adsorption capacity also increased (Table 2), suggesting that the adsorption process is endothermic. The increase in adsorption capacity may also be a result of increased phenol mobility with increasing temperature [17]. According to [18], with temperature increase, pollutant solubility also increases, facilitating the entry of adsorbate into the asorbent's micropores.

#### 3.2.2. Kinetic modeling

The evaluation of kinetic models was performed through analysis of coefficients of determination ($R^2$) and by the proximity of experimental data and data predicted by the kinetic models. The pseudo-second order model adjusted better for most tests. According to [19], the pseudo-second order model indicates that the chemisorption is possibly the predominant reaction mechanism between adsorbent and adsorbate. These author's results, with phosphate adsorption by activated carbon, also were better adjusted to the pseudo-second order model.

#### 3.2.2. $H_2O_2$/UV

Fig. 2 shows the kinetic curves of phenol oxidation by $H_2O_2$/UV in the different experimental conditions.

The concentration of $H_2O_2$ had a positive effect on phenol removal. In contrast, pH did not have a significant effect. Under alkaline conditions (pH 11), degradation degree was lower than in acidic (pH 3). This influence is confirmed by the statistical analysis shown in Fig. 3, where it is observed that the higher the concentration in $H_2O_2$, the higher is the elimination rate; and the opposite is observed with lower pH.

Table 2
Adsorption capacities (mg/g) obtained from adsorption kinetics for each of the tests

| Test | Activated carbon mass (g) | pH | Temperature (°C) | Adsorption capacity (mg/g) |
|---|---|---|---|---|
| 1 | 0.2 | 3 | 15 | 16.78 |
| 2 | 0.6 | 3 | 15 | 15.93 |
| 3 | 0.2 | 11 | 15 | 63.39 |
| 4 | 0.6 | 11 | 15 | 36.78 |
| 5 | 0.2 | 3 | 45 | 45.19 |
| 6 | 0.6 | 3 | 45 | 24.32 |
| 7 | 0.2 | 11 | 45 | 67.37 |
| 8 | 0.6 | 11 | 45 | 30.79 |
| 9 | 0.4 | 7 | 30 | 34.22 |
| 10 | 0.4 | 7 | 30 | 39.38 |
| 11 | 0.4 | 7 | 30 | 30.58 |

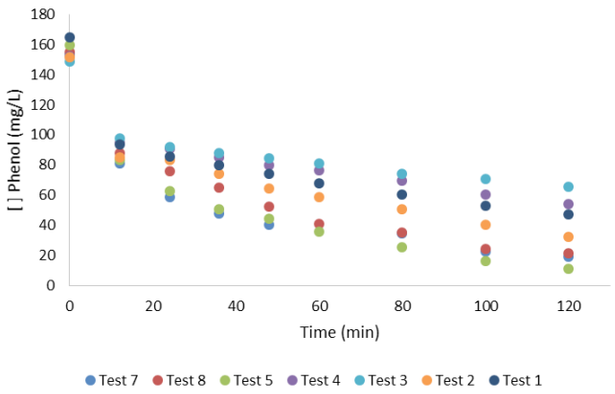


Fig. 2. Oxidation Kinetics: 10 mmol $H_2O_2$, pH 3 (• Test 1); 30 mmol $H_2O_2$, pH 3 (• Test 2); 10 mmol $H_2O_2$, pH 11 (• Test 3); 30 mmol $H_2O_2$, pH 11 (• Test 4); 20 mmol $H_2O_2$, pH 7 (• Test 5, • Test 6 and • Test 7).

At 20 mmol and pH 7 (tests 5, 6 and 7), the highest rates of phenol removal were obtained with rates of 93.01%, 86.26% and 87.69%, respectively. According to reaction 1, $H_2O_2$ can work as a hydroxyl radical receptor. Therefore, if it is in excess, as in tests 3 and 4 (30 mmol $H_2O_2$), the efficiency of photocatalytic reaction (12) is going to decrease, as occurred in the present experiments.

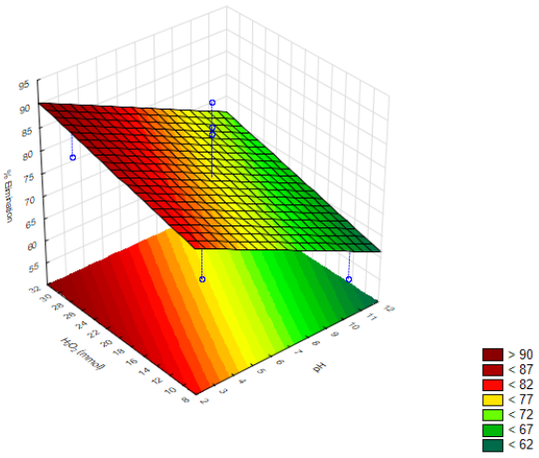


Fig. 3. Response surface of the $H_2O_2$/UV process, considering pH vs. $H_2O_2$ concentration.

$$OH + H_2O_2 \rightarrow HO_2 + H_2O \quad (12)$$

The activated carbon micrographs resulting from the $H_2O_2$/UV/activated carbon process (pH 7 and 20 mmol $H_2O$) (a) and crude activated carbon (b) are shown in Figs. 4 and 5. It is possible to observe that the crude activated carbon has an irregular surface structure.

Mathematical modeling of the kinetics of $H_2O_2$/UV process was performed for determination of $k_{homogeneous}$. According to Table 3, kinetic constants decreased as pH and determination coefficients ($R^2$) increased. Under these conditions, according to the phenol elimination rate, the first order kinetic constants found for the best condition (tests 5, 6 and 7) were similar to those found by [20].

The kinetic constants decreased with the increase of pH from 3 to 11, as well as determination coefficients ($R^2$). Under these conditions the best kinetic constants were in the central experiments [21]. Also found the best removal rate without pH 7, as well as kinetic constants very close

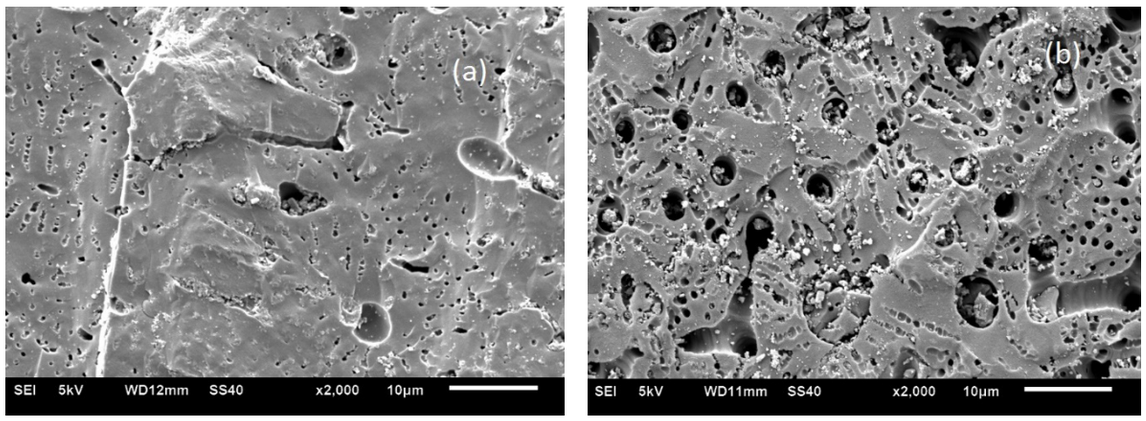


Fig. 4. SEM images with 2000× magnification of the activated carbons (a) resulting from the process with $H_2O_2$/UV and (b) crude.

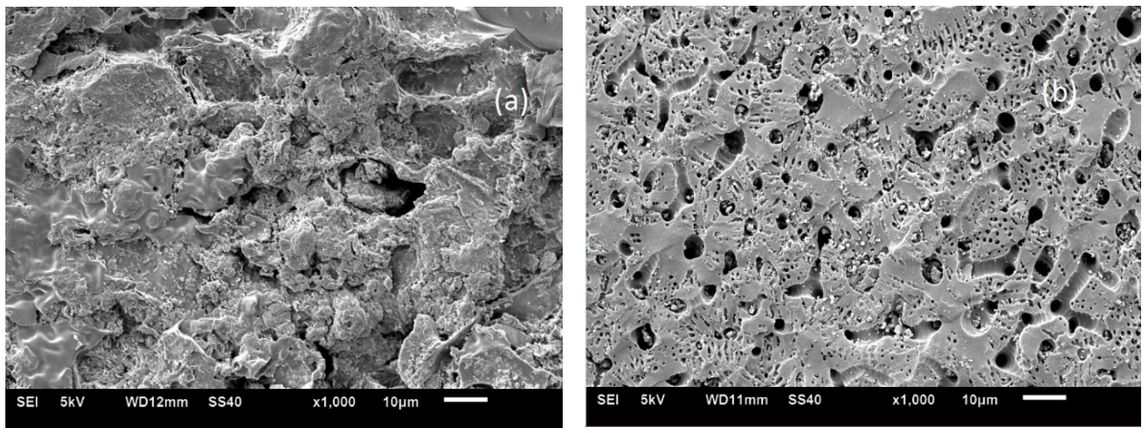


Fig. 5. SEM Images with 1000× magnification of the activated carbons (a) resulting from the process with $H_2O_2$/UV and (b) crude.

Table 3
First order kinetic constants and determination coefficients ($R^2$) for the tests performed in $H_2O_2$/UV treatment

| Test | ph | $H_2O_2$ concentration (mmol) | $k_{homogeneous}$ ($min^{-1}$) | $R^2$ |
|---|---|---|---|---|
| 1 | 3 | 10 | 0.0084 | 0.8478 |
| 2 | 3 | 30 | 0.0108 | 0.9277 |
| 3 | 11 | 10 | 0.0052 | 0.7785 |
| 4 | 11 | 30 | 0.0068 | 0.8503 |
| 5 | 7 | 20 | 0.02 | 0.9725 |
| 6 | 7 | 20 | 0.0155 | 0.9581 |
| 7 | 7 | 20 | 0.0149 | 0.8976 |

to those found in the present work [20] also found kinetic counters 0.0163, 0.0141 and 0.0171 $min^{-1}$ in the removal of phenolic compounds by the $H_2O_2$/UV process.

### 3.2.4. $H_2O_2$/UV/AC

Fig. 6 illustrates phenol oxidation kinetics by $H_2O_2$/UV/Activated carbon in different experimental conditions.

The effects of parameters in coupling were very similar to the effects of $H_2O_2$/UV process. The central points (tests 5, 6 and 7) were the best conditions for the $H_2O_2$/UV process, which presented removal rates of 86.29%, 87.69% and 93.01%, respectively. When the activated carbon was added in the coupling process, these values increased to 92.76%, 93.32% and 96.41%.

One way to analyze the degradation pathways is by calculating the kinetic contribution mechanism (δ). In Table 4, the results of the kinetic contributions show that phenol degradation is predominant in the homogeneous phase, but a part occurs at the surface of activated carbon, showing that it contributes significantly to the increase of phenol removal rate. The experimental results are consistent with the literature [22,23], which suggests that the presence of oxygen groups on the sorbent surface do CA causes an increase in the efficiency of $H_2O_2$decomposition and contributes to hydroxyl radicals generation.

The kinetic constants decreased with pH increase from 3 to 11, and determination coefficients ($R^2$) were higher than those found in the $H_2O_2$/UV process, since degradation rates were also higher. Under these conditions the best kinetic constants obtained were in the central experiments (5, 6 and 7) according to the phenol elimination rate, were 0.0237, 0.02 and 0.0207 $min^{-1}$.

Phenol degradation (molecular or radical) was studied to better understand the impact of activated carbon. For this experiment, a radical inhibitor, tert-butanol, applied to tests 5, 6 and 7 (central points of $H_2O_2$/UV/activated carbon) were applied to the coupling.

### 3.2.5. $H_2O_2$/UV/AC/tert-butanol

The $H_2O_2$/UV/Activated carbon/tert-butanol coupling kinetics curves are shown in Fig. 7 .

According Table 5, for the $H_2O_2$/UV/AC/tert-butanol treatment a phenol elimination rate of 66.75% was obtained

Table 4
First-order kinetic constants, determination coefficients ($R^2$) and kinetic contributions (δ) for the tests performed on $H_2O_2$/UV/activated carbon treatment

| Test | ph | $H_2O_2$ concentration (mmol) | $K_{global}$ ($min^{-1}$) | $R^2$ | $\delta_{homogeneous}$ | $\delta_{heterogenous}$ |
|---|---|---|---|---|---|---|
| 1 | 3 | 10 | 0.0118 | 0.9141 | 71.18 | 28.82 |
| 2 | 3 | 30 | 0.0173 | 0.9816 | 62.42 | 37.58 |
| 3 | 11 | 10 | 0.0059 | 0.7309 | 88.14 | 11.86 |
| 4 | 11 | 30 | 0.0086 | 0.713 | 79.07 | 20.93 |
| 5 | 7 | 20 | 0.0237 | 0.9597 | 84.39 | 15.61 |
| 6 | 7 | 20 | 0.0200 | 0.965 | 77.5 | 22.5 |
| 7 | 7 | 20 | 0.0207 | 0.9534 | 71.98 | 28.02 |

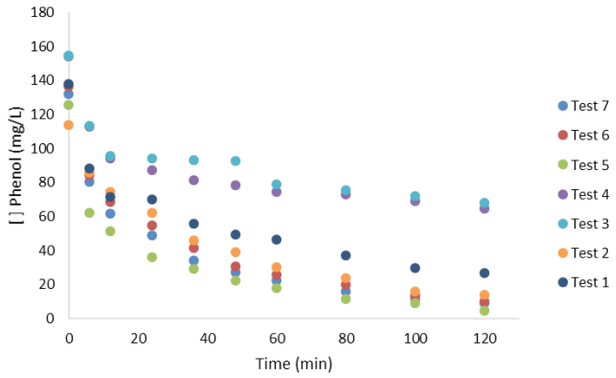


Fig. 6. Phenol concentration as a function of time for coupling process of $H_2O_2$/UV activated carbon: 10 mmol $H_2O_2$, pH 3 (● Test 1); 30 mmol $H_2O_2$, pH 3 (● Test 2); 10 mmol $H_2O_2$, pH 11 (● Test 3); 30 mmol $H_2O_2$, pH 11 (● Test 4);20 mmol $H_2O_2$, pH 7 (● Test 5,● Test 6 and ● Test 7, with 0.6g of activated carbon).

with a first order rate constant of 0.0048 $min^{-1}$, and the corresponding values in the absence of tert-butanol were 96.41% and 0.0237 $min^{-1}$. The reduction in kinetic constant brought a consequent reduction in phenol elimination rate, proving the inhibition by free radicals.

A graph was plotted for the calculation of kinetic constants (Fig. 8), neperian logarithm of the relative concentration of phenol versus time, where the first order kinetic constant is the angular coefficient of the line. For the $H_2O_2$/UV/AC treatment the constant is 0.0237 $min^{-1}$ and for the $H_2O_2$/UV/AC/tert-butanol treatment the constant is 0.0048 $min^{-1}$ and, consequently, the kinetic constant for contribution of ·OH radicals is the difference between them (0.0189 $min^{-1}$). The $\delta_{OH^\circ}$ radical contribution to the kinetic constants is 77.64%.

Radical contribution of $\delta_{OH^\circ}$ indicates that 79.74% of the phenol elimination in the $H_2O_2$/UV/activated carbon process was caused by the action of hydroxyl radicals and only 22.36% by the activated carbon adsorption [24] also found a significant radical contribution, 82% in the removal of benzothiazole by the use of $O_3$/activated carbon and the oxidative pathway is the main route of degradation of

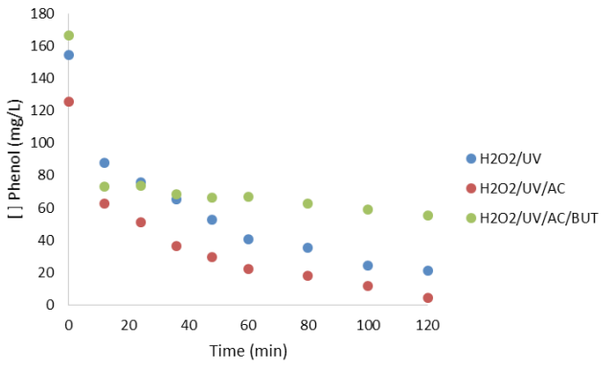


Fig. 7. Comparison between the kinetics of the $H_2O_2$/UV, pH 7 and 20 mmol $H_2O_2$ (●); $H_2O_2$/UV/ 0.6 activated carbon process, pH 7, 20 mmol $H_2O_2$ (●); and $H_2O_2$/UV/ 0.6 activated carbon/ 0.6 g/L of tert-butanol, pH 7, 20 mmol $H_2O_2$ (●).

Table 5
Comparison between the pseudo first order kinetic constants and elimination rates of the $H_2O_2$/UV, $H_2O_2$/UV/activated carbon and $H_2O_2$/UV/activated carbon /tert-butanol processes

| Treatment | $k$ ($min^{-1}$) | Elimination rate (%) |
|---|---|---|
| $H_2O_2$/UV | 0.0168 | 89.00 |
| $H_2O_2$/UV/activated carbon | 0.0237 | 94.16 |
| $H_2O_2$/UV/ activated carbon/tert-butanol | 0.0048 | 66.75 |

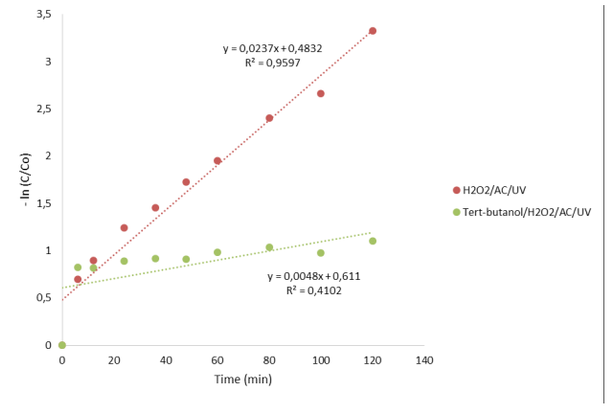


Fig. 8. Tert-butanol effect on phenol removal (●), experimental conditions: 0.6 g of activated carbon, 33 W, pH 7, [phenol] = 0.2 g/L, 30°C. Experiments without tert-butanol (●).

this element. There is activated carbon with 78.29% phenol removal, $H_2O_2$/UV with 89%, $H_2O_2$/UV/activated carbon with 94.16% and $H_2O_2$/UV/activated carbon/tert-butanol with 66.75%, where the coupling of an advanced oxidative process with activated carbon adsorption proved to be efficient in phenol elimination.

The experiment confirms that the attack of ·OH radicals is a very important mechanism involved in the degradation of phenol. Similarly, [25] observed that the removal of methylparation (20 mg/L) was inhibited by tert-butanol (1 g/L) under hydrodynamic cavitation and then confirmed that the degradation was dominated by free radical attack.

## 4. Conclusion

In the kinetics study, adsorption capacities were determined and the best test (pH 11, 45°C and 0.6 g activated carbon) obtained 30.79 $mg \cdot g^{-1}$ and this was chosen according to the statistical analysis. The pseudo-second order was the model that adjusted the most. Through the systems and the statistical analysis, an influence of the factors for the adsorption process is identified, being a positive effect of the temperature, positive effect by the pH and negative of the activated carbon mass, on the adsorption capacity.

For both treatments ($H_2O_2$/UV and $H_2O_2$/UV/AC), pH showed a negative release on elimination rate and $H_2O_2$ concentration presented a positive effect. The best tests for $H_2O_2$/UV and $H_2O_2$/UV/AC were the center points (pH 7 and 20 mmol $H_2O_2$) with phenol elimination rates of 89% and 94.16%, respectively. The kinetic contribution of hydroxyl radicals was calculated with the presence of a free radical inhibitor (tert-butanol) showing that 77.64% phenol elimination without $H_2O_2$/UV/AC treatment was caused by the action of hydroxyl radicals. The $H_2O_2$/UV/CA coupling process proved to be acceptable, presenting a higher removal rate than the adsorption process with a shorter removal time. Nevertheless, it is necessary to perform an economic viability analysis about the addition of activated carbon in the treatment system proposed by this study.

## Symbols

$\delta_{homogeneous}$ — Kinetic contribution of the homogeneous phase (%)
$\delta_{heterogeneous}$ — Kinetic contribution of the homogeneous phase (%)
$k_{heterogeneous}$ — First-order kinetic constant of the heterogeneous phase ($min^{-1}$)
$k_{homogêneous}$ — First-order kinetic constant of the homogeneous phase ($min^{-1}$)
$k_{global}$ — Represents the global reaction constant in the heterogeneous and homogeneous phase ($min^{-1}$)
$k_{global\ obs}$ — First-order kinetic constant of tert-butanol ($min^{-1}$)
$q_e$ — Amount of solute adsorbed by unit mass of adsorbent ($mg \cdot g^{-1}$); $C_0$ and $C_e$ ($mg \cdot L^{-1}$) are the initial and final concentrations of the adsorbent in the liquid phase, respectively
$V$ — Volume of solution (L)
$M$ — Adsorbent mass (g)
$q_e$ — Amount of solute adsorbed per unit mass of adsorbent ($mg \cdot g^{-1}$)
$q_t$ — Amount of solute adsorbed per unit mass of adsorbent ($mg \cdot g^{-1}$) at time t (min)
$k_1$ — Kinetic constant of pseudo-first order ($min^{-1}$)
$k_2$ — Kinetic constant of pseudo-second order ($g \cdot mg^{-1} \cdot min^{-1}$)

$k_3$ — Intraparticle diffusion kinetic constant ($mg \cdot g^{-1} \cdot min^{-0.5}$)

$c$ — Constant related to the thickness of the internal or external diffusion layer ($mg \cdot g^{-1}$)

**Acknowledgements**

To FAPEG (Goias State Research Support Fondation) for the scholarship, to FBC (Fabrica Brasileira de Catalisadores), which provided the activated carbon and to the Faculty of Chemical Sciences of the University of Salamanca in Spain, for the partnership and conducting of $N_2$ Adsorption/Desorption analysis.

**References**

[1] U. Beker, B. Ganbold, H. Dertli, D.D. Gulbayir, Adsorption of phenol by activated carbon: Influence of activation methods and solution pH, Energ. Convers. Manage., 51 (2010) 235–240.
[2] I. Ipek, N. Kabay, M. Yuksel IPEK, Separation of bisphenol A and phenol from water by polymer adsorbents: Equilibrium and kinetics studies, J. Water Process Eng., 16 (2017) 206–211.
[3] V.K. Gupta, M. Sharma, K. Singh, R.K. Vyas, Reactive adsorption of phenol onto Fe-GAC: Parallel pore batch modeling and experimental studies, J. Taiwan Inst. Chem. E., 63 (2016) 116–124.
[4] M. Pera-Titus, V. Garcia-Molina, M.A. Barros, J. Gimenez, S. Esplugas, Degradation of chlorophenols by means of advanced oxidation processes: A general review. Appl. Catal. B: Environ., 47 (2004) 219–256.
[5] H.F. Stoeckli, (1995) In: Porosity in Carbons – Characterization and Applications, Patrick, J. ed.; Arnold: London, p. 67–92.
[6] H.F. Stoeckli, M.V Lopez-Ramon, D. Hugi-Cleary, A. Guillot Micropore sizes in activated carbons determined from Dubinin–Radushkevich equation, Carbon, 39 (2001) 1115–1116.
[7] H.P. Boehm, Surface oxides on carbon and their analysis: A critical assessment, Carbon, 40 (2002) 145–149.
[8] J.R. Regalbuto, J.O. Robles, The Engineering of Pt/Carbon Catalyst Preparation. University of Illinois, Chicago, 2004, 13.
[9] S. Lagergren, On the theory of so-called adsorption dissolved substances, Handlingar Band, 24 (1898) 1–39.
[10] Y.S. Ho, D.A.J. Wase, C.F. Forster, Kinetic studies of competitive heavy metal adsorption by sphagnum moss peat, Environ. Technol., 17 (1996) 71–77.
[11] W.J. Weber, J.C. Morris, Kinetics of adsorption on carbon from solution, J. Sanitary Engng, Division ASCE, 89 (1963) 31–60.
[12] P.N. Patil, P.R. Gogate, Degradation of methyl parathion using hydrodynamic cavitation: Effect of operating parameters and intensification using additives, Sep. Purif. Technol., 95 (2012) 172–179.
[13] D.L. Pavia, G.M. Lampman, G.S. Kriz, Introduction to Spectroscopy third edition, Thomson Learning, Inc., 2001.
[14] E.L. Scheneider, Adsorption of phenolic compounds on activated carbon, Universidade Estadual do Oeste do Paraná, Brasil, 2008.
[15] S. Al-Asheh, F. Banat, L. Abu-Aitah, Adsorption of phenol using different types of activated bentonites, Sep. Purif. Technol., 33 (2003) 1–10.
[16] A. Islam, M.J. Ahmed, W.A. Khanday, M. Asif, B.H. Hameed, Mesoporous activated carbon prepared from NaOH activation of rattan (Lacosperma secundiflorum) hydrochar for methylene blue removal, Ecotox. Environ. Safe., 138 (2016) 279–285.
[17] M. Alkan, M. Dogan, Adsorption kinetics of Victoria blue onto perlite, Fresenius Environ. Bull., 12 (2003) 418–425.
[18] I.A. Mezzari, Use of adsorvent coal treatment of effluents containing pesticides, Federal university of Santa Catarina. 2002.
[19] W. Xiong, J. Tong, Z. Yang, G. Zeng, Y. Zhou, D. Wang, Adsorption of phosphate from aqueous solution using iron-zirconium modified activated carbon nanofiber: Performance and mechanism, J. Colloid. Interf. Sci., 493 (2017) 17–23.
[20] A. Zhang, Y. Li, Science of the total environment removal of phenolic endocrine disrupting compounds from waste activated sludge using UV, $H_2O_2$, and UV/$H_2O_2$ oxidation processes: Effects of reaction conditions and sludge matrix, Sci. Total Environ., 493 (2014) 307–323.
[21] A. Karci, I. Arslan-Alaton, M. Bekbolet, Advanced oxidation of a commercially important nonionic surfactant: investigation of degradation products and toxicity, J. Hazard. Mater., 263 (2013) 275–282.
[22] L. Dąbek, E. Ozimina, A. Picheta-Oleś, Dye removal efficiency of virgin activated carbon and activated carbon regenerated with Fenton`s reagent, Environ. Protect. Eng., 38 (2012) 5–13.
[23] L. Dąbek, E. Ozimina, A. Picheta-Oleś, Assessing the influence of the presence of heavy metals adsorbed on activated carbon on the efficiency of degradation of phenol using selected oxidizing agents, Soc. Ecol. Chem. Eng. S., 19 (2012) 249–257.
[24] Z.C. Kadirova, K. Katsumata, T. Isobe, N. Matsushita, A. Nakajima, K. Okada, Adsorption and photodegradation of methylene blue with $Fe_2O_3$-activated carbons under UV illumination in oxalate solution, J. Environ. Chem. Eng., 2 (2014) 2026–2036.
[25] C.A. Zaror, H. Valdés, Heterogeneous and homogeneous catalytic ozonation of benzothiazole promoted by activated carbon: Kinetic approach, Chemosphere, 65 (2006) 1131–1136.